ELSEVIER
Journal of Medical Imaging and Radiation Sciences xxx (xxxx) xxx
Journal of Medical Imaging and Radiation Sciences
Journal de l'imagerie médicale et des sciences de la radiation
www.elsevier.com/locate/jmir

Research Article

An assessment of the dose and image quality difference between AP and PA positioned adult radiographic knee examinations

P. Lockwood [1,*] and M. Mitchell [1,2]

[1] *School of Allied Health Professions, Faculty of Medicine, Health and Social Care, Canterbury Christ Church University, Kent, United Kingdom*
[2] *Imaging Department, Medway Maritime Hospital, Medway NHS Foundation Trust, Gillingham, Kent, United Kingdom*

Available online xxx

ABSTRACT

Introduction: Knee X-rays are a standard examination to diagnose multiple conditions ranging from traumatic injuries, degeneration, and cancer. This study explores the differences between adult Anterior-Posterior (AP) and Posterior-Anterior (PA) weight-bearing knee examinations using absorbed radiation dose data and image quality.

Methods: The study modelled and compared AP and PA knee X-ray radiation dose data using Monte-Carlo software, an Ion Chamber, and thermoluminescence dosemeters (TLDs) on a Rando phantom. Imaging parameters used were 66kVp, 4mAs, 100cm distance and 13 × 24cm collimation. The interval data analysis used a two-tailed *t*-test. The image quality of a sample of the AP and PA knee X-rays was assessed using Likert 5-point ordinal Image Quality Scoring (IQS) and the Wilcoxon matched pairs test.

Results: Monte-Carlo modelling provided limited results; the Ion Chamber data for absorbed dose provided no variation between AP and PA positions but was similar to the AP TLD dose. The absorbed doses recorded with batches of TLDs demonstrated a 27.4% reduction (46.1μGy; p=0.01) in Skin Entrance Dose (ESD) and 9 - 58% dose reduction (1.6 – 16.4μGy; p=0.00-0.2) to the tissues and organs while maintaining diagnostic image quality (p=0.67).

Conclusion: The study has highlighted the various challenges of using different dosimetry approaches to measure absorbed radiation dose in extremity (knee) X-ray imaging. The Monte-Carlo simulated absorbed knee dose was overestimated, but the simulated body organ/tissue doses were lower than the actual TLD absorbed doses. The Ion Chamber absorbed doses did not differentiate between the positions. The TLD organ/tissue absorbed doses demonstrated a reduction in dose in the PA position compared to the AP position, without a detrimental effect on image quality. The study findings in laboratory conditions raise awareness of opportunities and potential to lower radiation dose, with further study replicated in a clinical site recommended.

Résumé

Introduction: Les radiographies du genou sont un examen standard pour diagnostiquer de multiples conditions allant des blessures traumatiques à la dégénérescence et au cancer. Cette étude explore les différences entre les examens du genou en appui sur le poids chez l'adulte en position antéro-postérieure (AP) et postéro-antérieure (PA) en utilisant les données sur la dose de rayonnement absorbée et la qualité de l'image.

Méthodologie: L'étude a modélisé et comparé les données de dose de rayonnement X du genou AP et PA en utilisant le logiciel Monte-Carlo, une chambre d'ionisation et des dosimètres à thermoluminescence (DTL) sur un fantôme Rando. Les paramètres d'imagerie utilisés étaient les suivants : 66kVp, 4mAs, distance de 100cm et collimation de 13 × 24cm. La qualité d'image d'un échantillon des radiographies AP et PA du genou a été évaluée à l'aide d'un score ordinal de qualité de l'image (IQS) selon une échelle de Likert en 5 points.

Contributors: All authors contributed to the conception or design of the work, the acquisition, analysis, or interpretation of the data. All authors were involved in drafting and commenting on the paper and have approved the final version.

Funding: This study did not receive any specific grant from funding agencies in the public, commercial, or not-for-profit sectors.

Competing interests: All authors declare no conflict of interest. The main author was the principal researcher in diagnostic radiography at Canterbury Christ Church University.

Ethical approval: Institutional ethical approval was received for this study [ETH2021-0264]. Written informed consent was obtained for all IQS participants. No images were altered, electronically cropped, or post-process manipulated for the IQS evaluation.

* Corresponding author: School of Allied Health Professions, Faculty of Medicine, Health and Social Care, Canterbury Christ Church University, Kent, United Kingdom.

E-mail address: paul.lockwood@canterbury.ac.uk (P. Lockwood).

https://doi.org/10.1016/j.jmir.2022.12.004

Résultats: La modélisation de Monte-Carlo a fourni des résultats limités; les données de la chambre d'ionisation pour la dose absorbée n'ont fourni aucune variation entre les positions AP et PA mais étaient similaires à la dose AP du DTL. Les doses absorbées enregistrées avec les lots de DTL ont démontré une réduction de 27,4 % (46,1μGy; p=0,01) de la dose à l'entrée de la peau (ESD) et une réduction de 9 à 58 % de la dose (1,6 - 16,4μGy; p=0,00-0,2) aux tissus et organes tout en maintenant la qualité de l'image diagnostique (p=0,22-0,74).

Conclusion: Cette étude a mis en évidence les différents défis liés à l'utilisation de différentes approches de dosimétrie pour mesurer la dose de rayonnement absorbée dans l'imagerie radiologique des extrémités (genou). La dose absorbée simulée par Monte-Carlo pour le genou était surestimée, mais les doses simulées pour les organes/tissus du corps étaient inférieures aux doses absorbées réelles par DTL. Les doses absorbées par la chambre d'ionisation ne faisaient pas la différence entre les positions. Les doses absorbées par DTL pour les organes/tissus ont montré une réduction de la dose en position PA par rapport à la position AP, sans effet négatif sur la qualité de l'image. Les résultats de l'étude dans des conditions de laboratoire sensibilisent aux possibilités et au potentiel de réduction de la dose de rayonnement, et il est recommandé de poursuivre l'étude dans un site clinique.

Keywords: Knee; X-ray; Positioning; Monte Carlo method; Thermoluminescence dosimeters; Image Quality

Introduction

The National Health Service (NHS) England Diagnostic Imaging Dataset [1] reporting service delivery to improve patient outcomes [2,3] recorded 41.7 million imaging examinations between December 2020 and November 2021. Of these, 3.6 million occurred in November 2021, [1] with X-rays as the most common test (1.77 million) [1]. Knee X-rays are a standard examination to assess the bony structure for multiple conditions ranging from traumatic injuries, degenerative joint disease to cancer. The presenting patients come from many different patient pathways and referral routes and include every possible age range.

There is published literature investigating the image quality of the standard knee positioning of the Anterior-Posterior (AP) weight-bearing straight leg. Still, limited studies review the alternative Posterior-Anterior (PA) position. The majority of studies investigate flexed PA views, [4] 45 degrees [5] including the Rosenburg view (angling the tube 10-20 degrees), [6,7] 20-30 degrees (including Lyon Schuss views),[8–10] Fixed Flexion Views,[11,12] and semi-flexed Buckland-Wright views [13,14]. The evidence is best evaluated by the literature review of tibiofemoral joint space narrowing in degeneration using PA knee flexion by Duncan et al. [15] Supported by Vince, Singhania and Glasgow [16] whose survey of n=800 members of the British Orthopaedic Association (BOA) who preferred PA weight-bearing knee X-rays (82%), citing the superiority in demonstrating the alignment of the joint for degenerative change. The survey was repeated six years later by Bhatnagar et al. [17] with n=990 BOA members, and the preference had risen to 86%, although with an inclination for a 30-degree flexion of the knee.

The United Kingdom (UK) Ionising Radiation (Medical Exposure) Regulations [18] (IR(ME)R) require the 'practitioner' (radiographer in the UK; radiologic technologist, or medical radiation technologist internationally) to adhere to keeping radiation dose 'As Low As Reasonable Practicable' (ALARP) [19,20] reduces the risk of tissue reactions and stochastic effects. Current Diagnostic Reference Levels (DRLs) have been set within the UK [21] for knee x-ray exposures at 0.3 milligrays (mGy) Entrance Skin Dose (ESD) per image (mean of n=3,295 patients, at 61 (52-68) Kilovoltage (kV); 4 (1-125) milliampere-seconds (mAs) [22].

Very little has been studied on the variance between adult AP and PA straight leg knee X-ray dose [23]. The UK College of Radiographers (CoR) Research Priorities for the radiographic profession [24] has "dose optimisation", "image quality", "methods to reduce ionising radiation", and "evidence-based procedures" within their top ten priority of topics. The CoR Research Strategy [25] highlights the need for research so that "all patients undergoing diagnostic imaging deserve evidence-based practice to underpin their care".

This novel and original study aims to assess AP and PA weight-bearing straight leg knee X-ray positioning, evaluating radiation dose and image quality. Using a three-stage approach of virtual simulation of dose (Monte Carlo software) and real dose measurements with Ion Chambers and Thermoluminescent Dosimeters (TLDs). With a null hypothesis (H_0) of no change in dose/image quality between AP and PA positioning and an alternative hypothesis (H_1) there was a change in dose/image quality between AP and PA positioning.

Methods

Three stages of dose collection methods were used to obtain and compare data. The first stage acquired a virtual patient simulation using Monte-Carlo software (PCXMC 2.0[26]) to model the absorbed radiation doses between the two knee positions (AP and PA) using an adult mathematical hermaphrodite Cristy phantom [27] (default modelling of a 30-year-old male Euro-American [27]). PCXMC [26] uses simulations of the interactions of photons to matter, accounting for photoelectric absorption, coherent (Rayleigh) scattering, and incoherent (Compton) scattering, [28] correlating well with National Radiological Protection Board (NRPB) modelling data [29–32]. Monte-Carlo calculations then estimate the absorbed dose and effective (organ and whole-body) dose using International Commission on Radiological Protection [33] (ICRP) tissue weighting (W_R) factors and lifetime risk estimate of cancer

Please cite this article as: P. Lockwood and M. Mitchell, An assessment of the dose and image quality difference between AP and PA positioned adult radiographic knee examinations, Journal of Medical Imaging and Radiation Sciences, https://doi.org/10.1016/j.jmir.2022.12.004

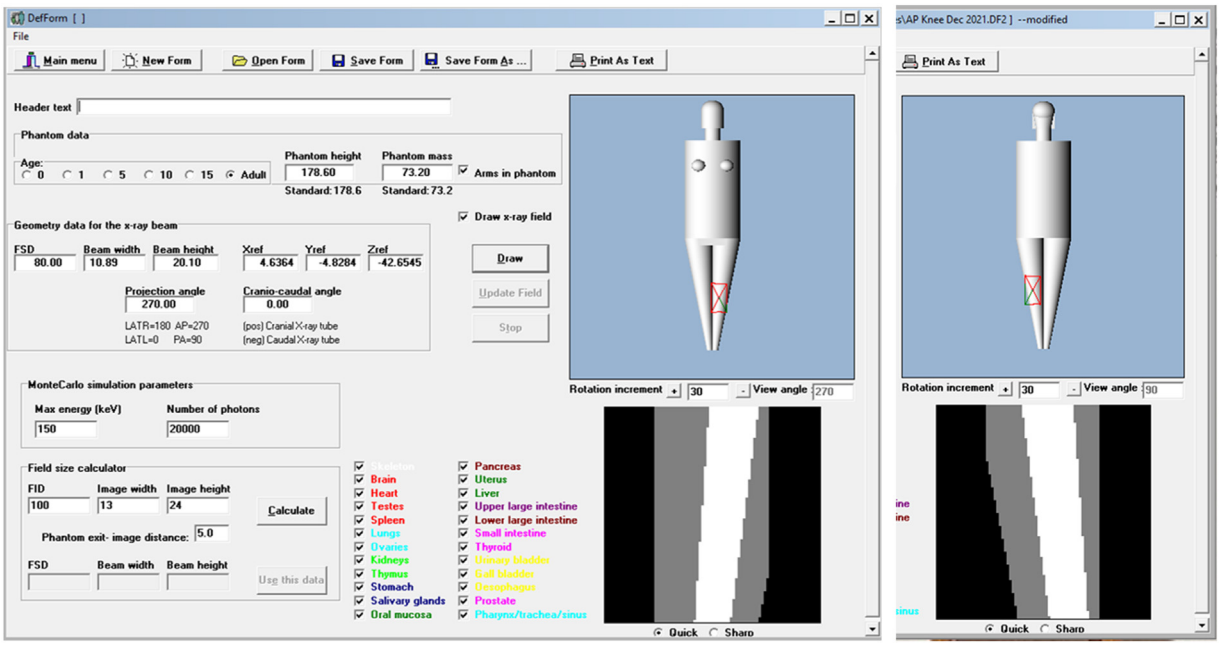

Fig. 1. Monte Carlo modelling using PCXMC[26] software of an AP (left image) and PA (right image) adult knee X-ray.

[34]. PCXMC [26] is designed for both localised anatomy and whole-body irritation simulations, thus, calculating the effective dose which is appropriate for whole-body irradiation [35]. In imaging examinations where a single organ (knee X-ray) receives the majority of doses, the mean absorbed doses should be used as the most appropriate quantity for organ and tissue doses as an indicator of deterministic effects [19]. The virtual patient simulation (Fig. 1) used adult knee imaging parameters (66kv, 4mAs, 100 centimeters (cm), source to image detector (SID), light beam collimation of 13 × 24cm, simulated Phantom height 178.6cm and mass 73.2 kilograms (kg).

The second stage assessment recorded real-world ESD from AP and PA knee X-ray examinations using a tissue equivalent male Alderson Rando phantom [36] and Ion Chamber [37] dosimeter [38] (Fig. 2) to determine the dose [39]. Positioning of the AP weight-bearing knee view followed clinical practice positioning, centring the horizontal beam 1cm below the apex of the patella through the joint space and collimated to include 1/3 of the tibia, fibula and femur [40]. For the PA weight-bearing positioning, the phantom was rotated 180 degrees, keeping the same X-ray tube centring position and SID, similar to the AP view [40]. The exposure factors used the local clinical X-ray protocol of 66kV, 4mAs, a small focal spot, a SID of 100cm, and collimation of 13 × 24cm set to the area of interest [40]. All X-ray equipment (X-ray tube [41], Direct Digital Radiography plate [42], Ion Chamber [37]) was quality assured at the start. Additionally, the Dose Area Product (DAP) meter data were recorded throughout the experiment to consistently monitor X-ray tube output.

Dosimetry studies routinely use a three-step process starting with recording the absorbed dose (micrograys (μGy), then manually calculate [33] (Fig. 3) the equivalent dose (based on

Fig. 2. Ion Chamber[37] positioning for AP skin entrance (absorbed) dose readings.

the average absorbed dose in the volume of a specified organ or tissue [19]) and then converted into units of microsieverts (μSv) and millisieverts (mSv) [43] for effective whole-body dose (harmful 'biological effect' of the X-rays photons) [19]. But effective dose estimates are only useful for comparing whole-body irradiation from different diagnostic modalities and techniques with different spatial distributions of radiation within body tissues [19].

The ICRP [19] recommend when considering exposures directed to a single organ (i.e. knee), mean absorbed doses should be used. The absorbed doses were recorded from three expo-

Please cite this article as: P. Lockwood and M. Mitchell, An assessment of the dose and image quality difference between AP and PA positioned adult radiographic knee examinations, Journal of Medical Imaging and Radiation Sciences, https://doi.org/10.1016/j.jmir.2022.12.004

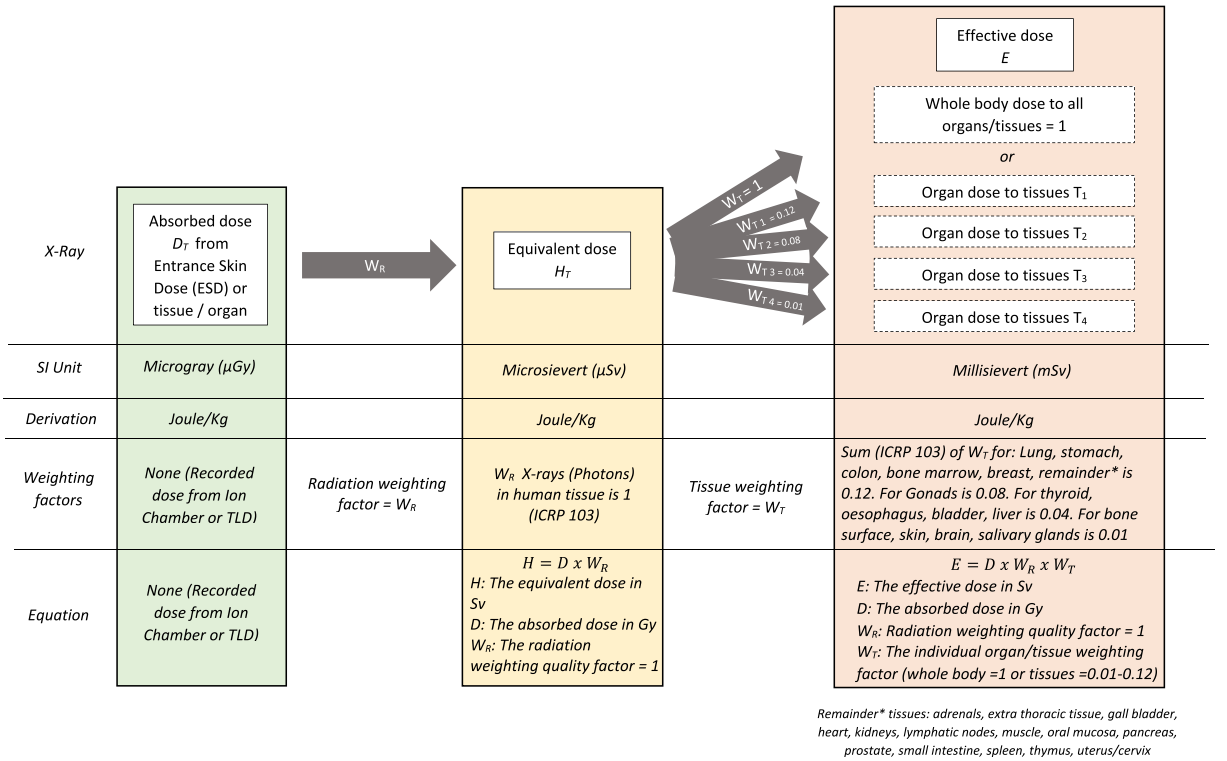

Fig. 3. Absorbed, equivalent and effective ionising radiation dose equations.[33]

sures taken consecutively at each projection to ensure the reliability of exposure output. This considered minor generator voltage fluctuation/ripple effect, electron kinetic energies across the tube, and any thermomechanical stress of the X-ray tube from previous usage.

The next stage used the same Alderson Rando [36] phantom, applying TLDs [44] to record real-world absorbed doses to the knee (ESD), skin exit, [28,38] adjacent limb, and the radiosensitive organs [33] (internal positioning holes between the assembled Rando [36] slices [28,33,38,45]) in both AP and PA positions (Figs. 4,5).

The TLDs [44] of Lithium Fluoride (LiF) crystals are tissue equivalent (Human tissue atomic number (Z) = 7.4, LiF Z = 8.2[28]). The manufacturing process causes microscopic crystal lattice imperfections and impurities [28] in the TLDs, acting as electron traps to capture the X-ray energy when irradiated. Thus, each TLD has minor variations and differences in sensitivity (light counts from the same X-ray irradiation) [46].

The TLDs were stored in a dark, temperature-controlled steel cupboard to reduce background radiation and sensitivity to daylight and fluorescent light [28]. Each TLD was moved using vacuum tweezers, as the surface coating of the TLDs is sensitive to the oil, grease, and associated dirt from human handling [28]. When read at high temperatures (242 degrees Celsius (°C), oil and grease ignite and give off a higher heat/light count value than the actual true value, giving false data [39]. Using vacuum tweezers further reduces the risk of dropping onto soiled surfaces, [39] causing fractures to the TLD structure and consequential errors in readings.

Fig. 4. TLDs[44] in batches of three positioned (N) as shown for ESD (absorbed) dose readings to the AP knee.

Before calibration, [47] the TLDs were annealed (242°C for 10 minutes, before rapidly cooling to 80°C for 20 minutes, before step cooled down) in an electric Carbolite Annealing oven [48]. This released any stored energy [38,48,49] in the TLD 'valence band' and re-combine the electrons and holes (traps) [50].

To reduce TLD variation in sensitivity (up to 10-30%), [46,49] n=100 TLDs were calibrated, by irradiating to the knee X-ray exposure, [26,37] on a tissue equivalent material (to reduce backscatter of low energy Compton X-rays [38])

Please cite this article as: P. Lockwood and M. Mitchell, An assessment of the dose and image quality difference between AP and PA positioned adult radiographic knee examinations, Journal of Medical Imaging and Radiation Sciences, https://doi.org/10.1016/j.jmir.2022.12.004

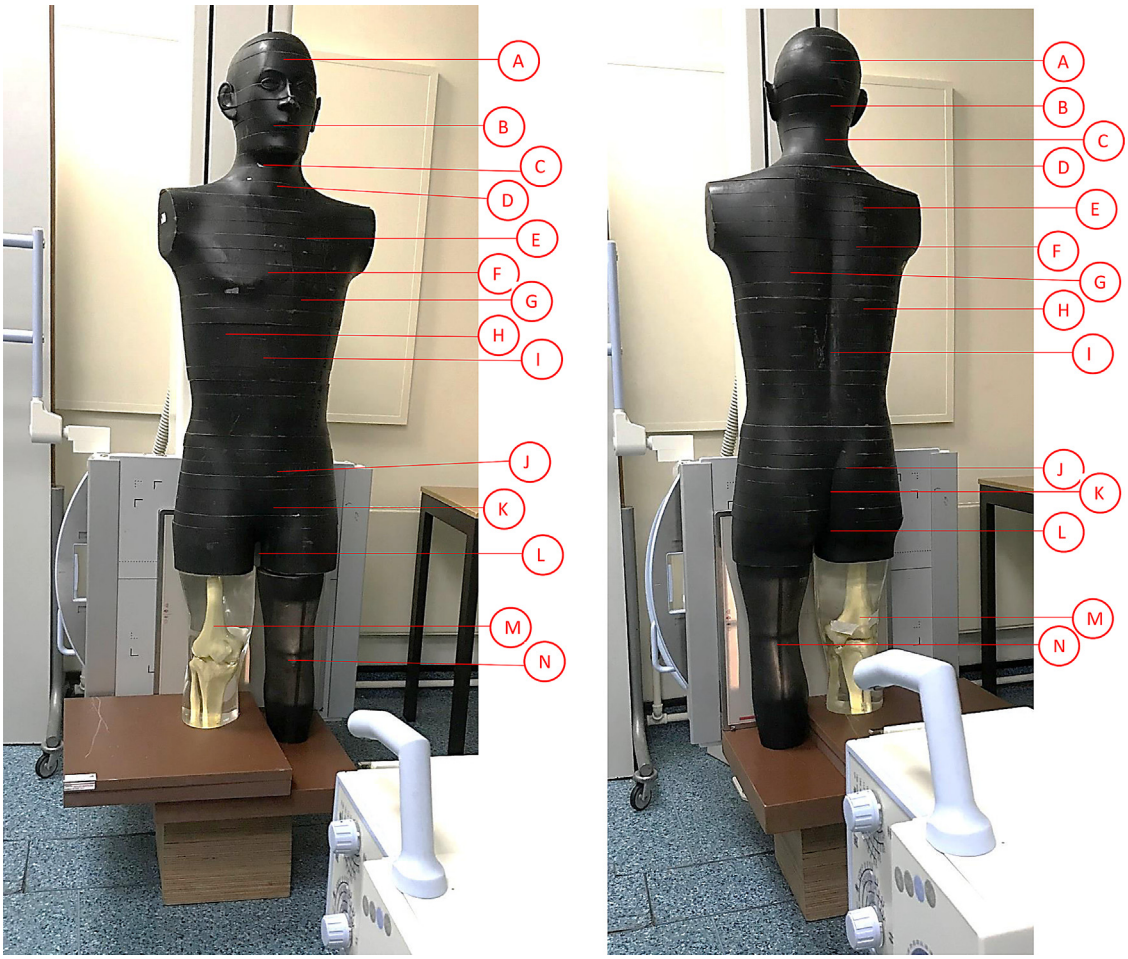

Fig. 5. AP and PA Alderson Rando[36] phantom standing on tissue-equivalent material displaying the positioning of TLDs[44] (A – Brain (Rando slice 1-2); B – Salivary glands (Rando slices 6-7); C – Oesophagus (Rando slice 8-9); D – Right and left thyroid (Rando slice 9-10); E - Right and left lung (Rando slice 15-16); F - Right and left breast (Rando slice 17-18); G - Stomach (Rando slice 19-20); H – Liver (Rando slice 20-21); I – Colon (Rando slice 23-24); J - Right and left ovaries (Rando slice 28-29); K- Bladder (Rando slice 32-33); L - Right and left testes (Rando slice 34-35); M – Right knee scatter (skin entrance and exit); N – Left knee primary beam (skin entrance and exit).

grouped within a 5-inch diameter circle [45]. The TLDs were then read and reordered into a sensitivity range [49] with the n=3 highest light counts (least variance) chosen for the experiment [50]. The mean light count from the batch of n=3 TLDs irradiated at each anatomical area in the phantom (in a reusable, re-sealable small plastic zip storage bag) to the same exposure and collimation as the PCXMC [26] and Ion Chamber [37] was recorded for the absorbed dose [19]. There were n=21 anatomical locations for the TLDs (Fig. 5), exposed and read, then repeated twice more in total n=126 exposures and readings of the TLD batch for the AP and PA positions.

After irradiation, the TLD reader [46] and software [51] use a Time/Temperature Profile (TTP) protocol [45,52] in a nitrogen atmosphere (purging the air during reading to reduce background radiation [47]) to preheat the TLDs (50°C) to remove shallow traps/low-temperature peaks [45]. Then fast heated (240°C) to acquire the high glow curve peaks [28] recorded in a generic unit (Nanocoulombs (nC), then the TLDs are fast annealed (quenched) to empty the traps [28,39,45,46].

The resulting light count (nC) data was then manually calculated (Fig. 6) as not auto-calibrated to a consistent local source of Caesium-137 or Strontium-90 [46]. Assessing the energy absorbed, minus the background radiation, [45] then converting the generic units (nC) to dose units (μGy), before calculating the mean absorbed dose from the batch of n=3 TLDs for each anatomical region.

The doses were presented in means with standard deviations (SD) [46] and analysed using inferential statistics of a two-tailed (direction of relationship) paired sample (AP vs PA) t-test to compare the mean ESD/absorbed dose for any statistically significant difference (chance or real effect using a p-value [55] (p) < 0.05 in hypothesis testing) difference between the AP and PA positioning. The two-tailed t-test [55] was chosen as TLD data is interval, and the hypothesis does not state which position would be higher/lower in dose.

The method to assess image quality used the Image Quality Scoring (IQS) [56] with Likert 5-point ordinal scales. A random selection of n=3 AP and n=3 PA knee X-ray im-

Please cite this article as: P. Lockwood and M. Mitchell, An assessment of the dose and image quality difference between AP and PA positioned adult radiographic knee examinations, Journal of Medical Imaging and Radiation Sciences, https://doi.org/10.1016/j.jmir.2022.12.004

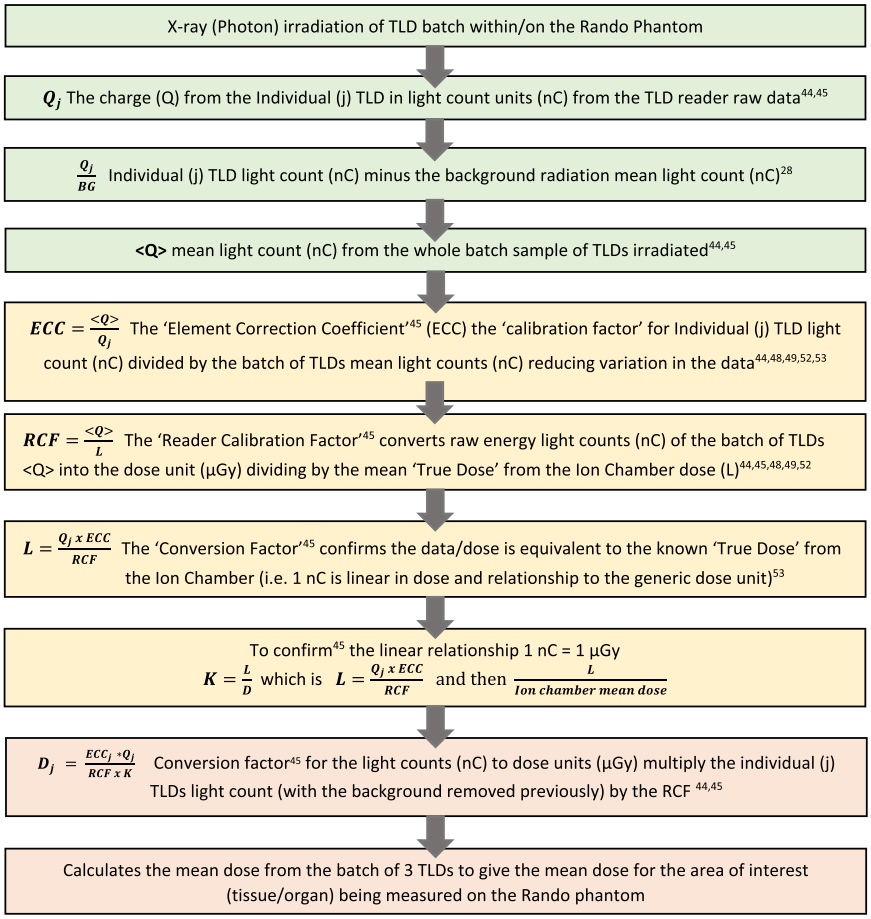

Fig. 6. TLD[44] light count generic unit (nC) to dose unit (Gy) element correction coefficients and calibration factors.[28,45,46,49,50,53,54]

ages from the TLD stage were randomly ordered (Random Sequence Generator [57]) to reduce bias [58] and presented on a Picture Archiving and Communication System (PACS) [59]. The participant criteria to evaluate the image quality used diagnostic radiographers (a sample of 3-10 radiographers are recommended [60–62]) independently blinded to each other's evaluation. The IQS ordinal data analysis applied a non-parametric Wilcoxon matched pairs test [55] (the equivalent of the two-tailed paired *t*-test), using $p < 0.05$, to test for statistical significance between the AP and PA knee image quality.

Institutional ethical approval was received for this study [ETH2021-0264]. Written informed consent was obtained for all IQS participants. No images were altered, electronically cropped, or post-process manipulated for the IQS evaluation.

Results

The PCXMC [26] Monte-Carlo modelling of the absorbed dose between the two positions (AP and PA) is displayed in Table 1. In the PA view, the average organ and tissue absorbed dose decreased by 3% (supplementary tables 1 and 2). The calculated stochastic radiation risk values [33] using the Risk of Exposure-induced Cancer Death (REID) metrics for the AP position was 4.7E-6% (0.0000047%) compared to the lower PA position of 4.24E-6% (0.0000042%). There was no difference in predicated remaining lifetime years (45.2 years) or estimated Loss of Life Expectancy (LLE) of 28.1 years using the imaging parameters and Cristy phantom [27] (age, weight).

The Ion Chamber [37] PA absorbed dose (169μGy; Tables 2,3) demonstrated a minor variance (59μGy) from the PCXMC [26] PA calculated absorbed dose (110μGy).

The TLD absorbed dose values determined with the Alderson Rando Phantom [36] (Table 4 and Fig. 7) indicated the PA positioning reduced the mean absorbed dose / ESD to the knee by 27.4% (46.1μGy; p=0.01) compared to the AP position. Further organ dose reductions using the PA position indicated a range of 9 - 58% (1.6 – 16.4μGy; p=0.00-0.28) to the tissues and organs compared to the AP position. Although not all p-values were significant, the exposed knee exit dose was 38% lower but p=0.07.

A comparison of the TLD AP position mean absorbed dose / ESD (168.1μGy) to the Ion Chamber [37] ESD (169.8μGy) displayed similar values, with the TLD PA position ESD lower (121.9μGy). Potential reasons include the TLD on the phantom surface in the AP position has the patella protruding from the skin surface toward the X-ray tube. In the PA position, the popliteal fossa indents the skin surface away, varying the distance slightly. In comparison, the Ion Chamber, [37] was a large size when in position on the skin surface, reducing distance variation.

Please cite this article as: P. Lockwood and M. Mitchell, An assessment of the dose and image quality difference between AP and PA positioned adult radiographic knee examinations, Journal of Medical Imaging and Radiation Sciences, https://doi.org/10.1016/j.jmir.2022.12.004

Table 1
PCXMC[26] Monte-Carlo modelling of tissue/organ absorbed dose (μGy) from the AP and PA position simulated adult knee X-ray.

	AP positioning		PA positioning		
ROI Anatomy	Dose (μGy)	Error (%)	Dose (μGy)	Error (%)	Dose change %
Upper leg bones	0.095	38.2	0.207	30.9	+117%
Middle leg bones	49.15	2.1	114.834	1.3	+133%
lower leg bones	340.694	0.9	248.967	1.2	-27%
Skin	42.389	1.0	31.382	0.9	-26%
Muscle	22.381	0.3	22.041	0.3	-1%
Testes	0.114	71.8	0.07	81.4	-38%
Bladder	0.00	N/A	0.11	100	0%
Ovaries	0.00	N/A	0.00	N/A	0%
Colon	0.00	N/A	0.003	81.2	0%
Liver	0.00	N/A	0.00	N/A	0%
Stomach	0.00	N/A	0.00	N/A	0%
Breasts	0.00	N/A	0.00	N/A	0%
Lung	0.00	N/A	0.00	N/A	0%
Thyroid	0.00	N/A	0.00	N/A	0%
Oesophagus	0.00	N/A	0.00	N/A	0%
Salivary gland	0.00	N/A	0.00	N/A	0%
Brain	0.00	N/A	0.00	N/A	0%

Table 2
Ion Chamber[37] AP knee absorbed and equivalent dose modelling using ICRP[33] weighting coefficients of biological effects of radiation type (WR = photons).

ROI Anatomy	Exposure	Absorbed Dose (μGy)	Equivalent Dose weightings	Equivalent Dose (μSv)
AP	1	169.8	x WR (1)	169.8
Skin Entrance Left Knee*	2	169.9	x WR (1)	169.9
	3	169.8	x WR (1)	169.8
	4	169.9	x WR (1)	169.9
	5	170	x WR (1)	170
	mean	169.88	mean	169.88

Table 3
Ion Chamber[37] PA knee absorbed and equivalent dose modelling using ICRP[33] weighting coefficients of biological effects of radiation type (WR = photons).

ROI Anatomy	Exposure	Absorbed Dose (μGy)	Equivalent Dose weightings	Equivalent Dose (μSv)
PA	1	169.8	x WR (1)	169.8
Skin Entrance Left Knee*	2	169.9	x WR (1)	169.9
	3	169.8	x WR (1)	169.8
	4	169.9	x WR (1)	169.9
	5	170	x WR (1)	170
	mean	169.88	mean	169.88

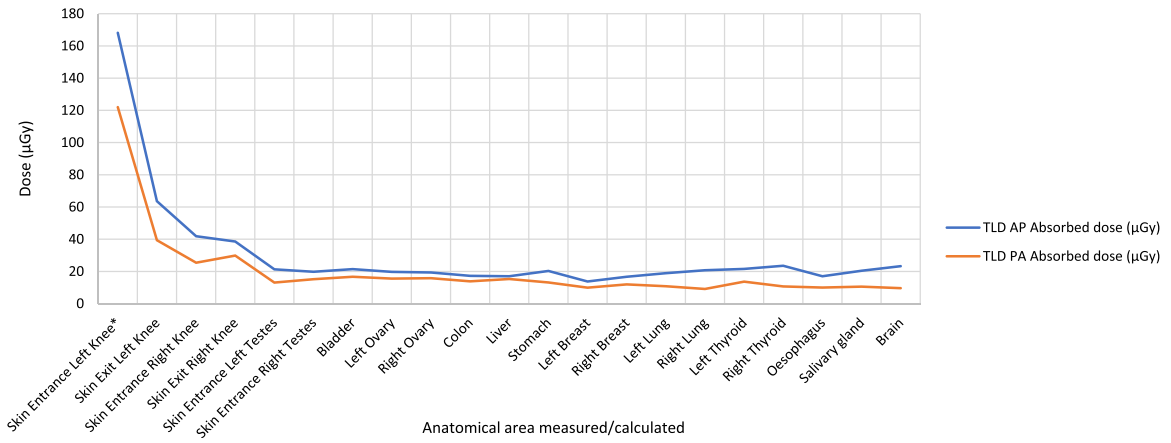

Fig. 7. Comparison of AP and PA positioned absorbed doses measured using TLDs.[44]

Please cite this article as: P. Lockwood and M. Mitchell, An assessment of the dose and image quality difference between AP and PA positioned adult radiographic knee examinations, Journal of Medical Imaging and Radiation Sciences, https://doi.org/10.1016/j.jmir.2022.12.004

Table 4
TLD[44] doses for the ICRP[33] radiation-sensitive organs, measured using the Alderson Rando Phantom.[36]

ROI Anatomy	AP Positioning					PA Positioning						
	Exposure 1 Mean TLD (μGy)	Exposure 2 Mean TLD (μGy)	Exposure 3 Mean TLD (μGy)	Mean Dose (μGy ±SD)	Conversion to mGy	Exposure 1 Mean TLD (μGy)	Exposure 2 Mean TLD (μGy)	Exposure 3 Mean TLD (μGy)	Mean Dose (μGy ±SD)	Conversion to mGy	Dose Change %	*t*-test *p*-value
Skin Entrance Left Knee*	174.14	157.54	172.68	168.12 ± 9.1	0.16	121.25	123.29	121.37	121.97 ± 1.1	0.12	-27.4%	p=0.016
Skin Exit Left Knee	70.61	68.88	51.3	63.59 ± 10.6	0.06	37.84	40.94	39.35	39.38 ± 1.5	0.03	-38%	p=0.072
Skin Entrance Right Knee	46.2	40.96	38.42	41.86 ± 3.9	0.04	26.13	22.16	27.88	25.39 ± 2.9	0.02	-39.3%	p=0.031
Skin Exit Right Knee	45.4	45.73	24.59	38.58 ± 12.1	0.03	32.2	26.94	30.34	29.83 ± 2.6	0.02	-22.68%	p=0.360
Skin Entrance Left Testes	18.94	22.67	22.24	21.28 ± 2.0	0.02	13.97	11.91	13.27	13.05 ± 1.0	0.01	-38.6%	p=0.040
Skin Entrance Right Testes	21.6	19.65	18.05	19.77 ± 1.7	0.01	16.01	14.28	15.24	15.17 ± 0.8	0.01	-23.3%	p=0.035
Bladder	19.01	25.03	20.27	21.43 ± 3.1	0.02	15.2	19.49	15.4	16.70 ± 2.4	0.01	-22%	p=0.011
Left Ovary	20.31	20.77	18.18	19.75 ± 1.3	0.01	15.7	15.27	15.67	15.54 ± 0.2	0.01	-21.3%	p=0.041
Right Ovary	20.6	22.74	14.72	19.35 ± 4.1	0.01	16.83	16.11	14.38	15.77 ± 1.2	0.01	-18.5%	p=0.187
Colon	17.41	15.87	18.43	17.24 ± 1.2	0.01	14.02	13.55	14.01	13.86 ± 0.2	0.01	-19.6%	p=0.030
Liver	19.51	15.07	16.41	16.99 ± 2.2	0.01	16.29	15.67	14.00	15.32 ± 1.1	0.01	-9.8%	p=0.285
Stomach	20.83	20.04	20.08	20.32 ± 0.4	0.02	13.14	14.55	11.66	13.12 ± 1.4	0.01	-35.4%	p=0.014
Left Breast	13.98	12.78	14.47	13.74 ± 0.8	0.01	9.6	9.87	10.28	9.92 ± 0.3	0.009	-27.8%	p=0.014
Right Breast	16.84	16.5	16.77	16.7 ± 0.1	0.01	11.83	12.58	11.39	11.93 ± 0.5	0.01	-28.5%	p=0.008
Left Lung	17.92	21.61	17.06	18.87 ± 2.4	0.01	11.7	11.3	9.51	10.78 ± 1.1	0.01	-42.8%	p=0.021
Right Lung	23.14	18.66	20.46	20.75 ± 2.2	0.02	8.41	9.09	9.82	9.11 ± 0.7	0.009	-56%	p=0.017
Left Thyroid	25.71	19.74	19.26	21.57 ± 3.5	0.02	15.37	12.54	13.06	13.66 ± 1.5	0.01	-36.7%	p=0.023
Right Thyroid	27.6	23.76	19.13	23.5 ± 4.2	0.02	11.21	10.33	10.49	10.68 ± 0.4	0.01	-54.5%	p=0.029
Oesophagus	17.32	16.08	17.53	16.97 ± 0.7	0.01	8.42	10.41	11.2	10.01 ± 1.4	0.01	-41%	p=0.019
Salivary gland	19.39	18.64	23.12	20.39 ± 2.3	0.02	10.44	11.5	9.73	10.56 ± 0.8	0.01	-48.2%	p=0.033
Brain	23.19	25.02	21.62	23.28 ± 1.7	0.02	8.48	11.62	8.7	9.60 ± 1.7	0.009	-58.7%	p=0.001
Skin Entrance Left Knee*	AP Mean Absorbed Dose 168.12μGy AP Mean Equivalent Dose (W_R) 168.12μSv					AP Mean Absorbed Dose 121.97μGy *AP Mean Equivalent Dose (WR) 121.97μSv*					-27.4%	p=0.016

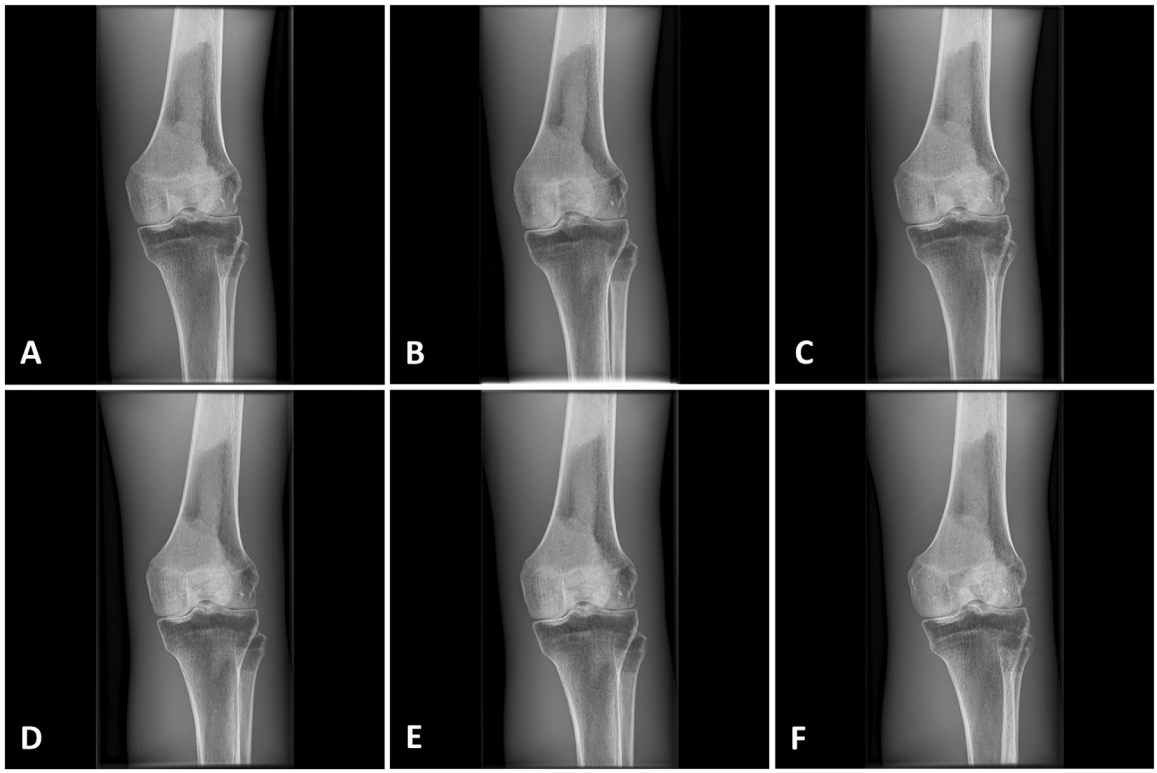

Fig. 8. AP positioned knee images (A, B, C), and PA positioned knee images (D, E, F).

Table 5
IQS[56] scores for AP and PA knee images, using a Wilcoxon matched pairs test, were statistically considered equivalent, with a small non-significant change in quality scores between them.

	AP Knee (A)	AP Knee (B)	AP Knee (C)	PA Knee (D)	PA Knee (E)	PA Knee (F)	Wilcoxon matched pairs test		
IQS Criteria	**Mean IQS ± SD**	**Mean IQS ± SD**	**Mean IQS ± SD**	**Mean IQS ± SD**	**Mean IQS ± SD**	**Mean IQS ± SD**	**SD**	***z-value***	***p*-value**
1.1 Visual sharpness of bone reproduction	3.4 ± 1.1	3.4 ± 1.2	3.4 ± 1.2	3.5 ± 0.9	3.2 ± 1.1	3.2 ± 1.1	1.02	z= 0.12	p=0.90
1.2 Subject contrast of the bones (femur, tibia, fibula, patella) with the adjacent soft tissue	3.4 ± 1.1	3.4 ± 1.2	3.4 ± 1.2	3.4 ± 1.2	3.5 ± 1.1	3.2 ± 1.3	0.44	z= -0.20	p=0.84
1.3 Signal to noise level	3.4 ± 1.1	3.1 ± 1.2	3.5 ± 1.2	3.1 ± 1.2	3.4 ± 1.1	3.2 ± 1.3	0.76	z= -0.29	p=0.77
Overall Mean	3.4 ± 0.0	3.3 ± 0.1	3.4 ± 0.0	3.3 ± 0.2	3.3 ± 0.1	3.2 ± 0.0	0.77	z= 0.42	p=0.67

The IQS assessment of image quality comparing the AP and PA positions was independently evaluated by n=7 radiographers with a mean experience of 25 years (13-40 years range) in image interpretation and image quality assessment. The n=6 images (Fig. 8) were reviewed in a random order without identifying the positioning, and the IQS (Table 5) inferred a small non-statistically significant change in quality scores between them (p=0.67).

Discussion

The PCXMC [26] simulated (Cristy phantom [27]) absorbed doses overestimated the dose to the lower leg (AP 340.6μGy; PA 248.9μGy) compared to the TLD (Alderson Rando Phantom [36]) recorded absorbed dose (AP 168.1μGy; PA 121.9μGy). In contrast, the Ion Chamber [37] recorded AP and PA absorbed doses were comparable (169.8μGy) and similar to the TLD AP absorbed knee dose (168.1μGy). But similar to the PCXMC [26] simulated PA absorbed dose, the Ion Chamber [37] recorded PA absorbed dose overestimated compared to the TLD PA recorded absorbed dose (121.9μGy). In summary, the PCXMC [26] simulation estimated the PA Knee was 27% lower absorbed dose than the AP position. The TLD recorded PA Knee absorbed dose was 27.4% lower than the AP position. Ion Chamber [37] recorded AP and PA knee absorbed doses were the same, possibly due to the Ion Chamber [37] sensitivity recording backscattered radiation as well as from the primary x-ray beam entering the phantom, unlike a

Please cite this article as: P. Lockwood and M. Mitchell, An assessment of the dose and image quality difference between AP and PA positioned adult radiographic knee examinations, Journal of Medical Imaging and Radiation Sciences, https://doi.org/10.1016/j.jmir.2022.12.004

solid-state detector; this may have increased the dose measurement.

The TLD (Alderson Rando Phantom [36]) recorded organ/tissue absorbed doses and calculated equivalent dose demonstrated a reduction in dose in the PA position compared to the AP position, without a detrimental effect on image quality (Table 5), due to a mixture of factors including moving anterior radiosensitive organs (thyroid, breast, testes, etc.) away from the direct primary beam.

There was a disparity when comparing the PCXMC [26] dose values to the TLD dose values. The exposure factor (4mAs) was possibly too low for the PCXMC [26] estimation of individual organ absorbed dose, resulting in minimal variance between the two positions. It has been reported [38] that Monte-Carlo calculations have inherent margins of error at low energies, and comparing PCXMC [26] simulated doses to real experiment doses has reported errors [26] of between 60%,[63] 30%[64] and 10% [65,66]. Potentially due to the approximation calculations, the finite amount of simulated photons, and/or phantom geometry differences.

The ICRP [19] recommend the absorbed dose as the most appropriate quantity to assess organ and tissue doses in terms of tissue reactions [19] from ionising radiation. The ICRP [19] propose a future move away from equivalent dose metrics to inform decisions on the justification of examinations. Current DRLs [21, 22] used within the NHS for knee X-ray imaging are 0.3mGy per X-ray (61kV and 4mAs), [21,22] although useful for optimisation of dose, it is based on a standard from groups of patients and not an individual patient dose (which may be higher or lower than the DRL) [35]. This study has shown that PA positioning dose (0.08mGy) was lower using 66kV and 4mAs.

These small-scale study findings within laboratory conditions are not generalisable to wider clinical radiology departments. However, these methods can be replicated in a clinical site for local decision making. The image quality assessment used a small sample of phantom images, which inferred a small non-statistically significant change in quality scores between AP and PA images (p=0.67). Future studies would benefit from clinical images being assessed to evaluate the ability of PA positioning to display subtle changes to the bone cortex and trabecular patterns in pathological conditions beyond degenerative joint changes, [4,5,8,10,11,13–17] such as tibial plateau fractures and any associated impact on diagnostic efficacy.

The ICRP [33] model of risk was calculated from Monte-Carlo calculations [67] for absorbed and effective dose that is roughly proportional to the 'radiation detriment' (subjectively combined risk of cancer induction, mortality from fatal cancer, and heritable effects). Limitations to this procedure are that nominal probability coefficients of the risks are made from simplified assumptions on ICRP [33,34] chosen organs and tissues, applying ICRP [33] rounded tissue weighting factors, which are averaged from seven long-running cancer registries (n=4 Asian, n=3 Euro-American [67,68] populations), and not specific to individual UK patients. The lifetime risk of cancer varies depending on the patient's organ, age, gender and population group, although at knee X-ray doses, the absolute risk reduction observed was low. Additionally, we acknowledge the associated uncertainties of effective dose (used in the PCXMC [26] estimation) as an approximate indicator for risk-adjusted estimates related to the probability of health determinates (stochastic effects) that rely on the Linear-non-Threshold (LNT) model, which has known errors of up to 40% [19]. Conversely, the study has not modelled the data to paediatric knee X-rays, of which the risk estimation would be higher.

The Monte-Carlo simulated dose and risk assessment are dependent upon the age, sex and weight of the virtual phantom [27] and the imaging parameters. The Ion Chamber [37] and TLDs used specific imaging parameters and phantom, [36] variations of these methods will result in different output data. Likewise, image dose and image quality vary between manufacturers and products; thus, the results are directly translatable only to the equipment used.

Conclusions

The study findings raise awareness of opportunities and potential to lower radiation absorbed dose using a PA weight-bearing straight-leg position to the knee by 27.4% (TLD absorbed dose difference of 46.1μGy; p=0.01) and 9 - 58% (1.6 – 16.4μGy; p=0.00-0.28) to whole-body tissues and organs (H_1) while maintaining diagnostic image quality (p=0.22-0.74; H_0) using an adult phantom. The data highlighted the various challenges of using different dosimetry approaches to record dose from extremity (knee) X-ray imaging and raises awareness of the possibilities and feasibilities to lower radiation dose. Further study of PA knee examinations replicated in a clinical site is advised. Additionally, future studies on other common AP positioned musculoskeletal X-ray examinations to evaluate alternative PA positioning (such as non-trauma spinal imaging) to reduce patient radiation dose are recommended.

Supplementary materials

Supplementary material associated with this article can be found, in the online version, at doi:10.1016/j.jmir.2022.12.004.

References

[1] NHS England and NHS Improvement. Diagnostic Imaging Dataset Statistical Release: Provisional monthly statistics, November 2020 to November 2021 , London; 2022.
[2] NHS England. Improving Outcomes: A Strategy for Cancer , London; 2011.
[3] NHS England. Achieving World-Class Cancer Outcomes: Taking the strategy forward, London; 2016.
[4] Farrugia Wismayer E, Zarb F. Radiography of the knee joint: A comparative study of the standing partial flexion PA projection and the standing fully extended AP projection using visual grading characteristics (VGC). *Radiography*. 2016;22(2):152–160. doi:10.1016/j.radi.2015.10.002.
[5] Devin G, Feibel R, Rody KGJ. 3-foot standing AP vs 45 degrees PA radiograph for OA of the knee. *Clin J Sport Med*. 2001;11(1):10–16.

Please cite this article as: P. Lockwood and M. Mitchell, An assessment of the dose and image quality difference between AP and PA positioned adult radiographic knee examinations, Journal of Medical Imaging and Radiation Sciences, https://doi.org/10.1016/j.jmir.2022.12.004

[6] Inoue S, Nagamine R, Miura H, Urabe K, Matsuda S, Sakaki K, et al. Anteroposterior weight-bearing radiography of the knee with both knees in semiflexion, using new equipment. *Journal of Orthopaedic Science*. 2001;6(6):475–480. doi:10.1007/s007760100000.
[7] Fontboté RC, Nemtala UF, Contreras OO, Guerrero R. Rosenberg projection for the radiological diagnosis of knee osteoarthritis. *Rev Med Chil*. 2008;136(7):880–884.
[8] Merle-Vincent F, Vignon E, Brandt K, Piperno M, Coury-Lucas F, Conrozier T, et al. Superiority of the Lyon schuss view over the standing anteroposterior view for detecting joint space narrowing, especially in the lateral tibiofemoral compartment, in early knee osteoarthritis. *Ann Rheum Dis*. 2007;66(6):747–753. doi:10.1136/ard.2006.056481.
[9] Vignon E, Piperno M, le Graverand M-PH, Mazzuca SA, Brandt KD, Mathieu P, et al. Measurement of radiographic joint space width in the tibiofemoral compartment of the osteoarthritic knee: Comparison of standing anteroposterior and Lyon Schuss views. *Arthritis Rheum*. 2003;48(2):378–384. doi:10.1002/art.10773.
[10] Rueckl K, Boettner F, Maza N, Runer A, Bechler U, Sculco P. The posterior–anterior flexed view is better than the anterior–posterior view for assessing osteoarthritis of the knee. *Skeletal Radiol*. 2018;47(4):511–517. doi:10.1007/s00256-017-2815-2.
[11] Kan H, Arai Y, Kobayashi M, Nakagawa S, Inoue H, Hino M, et al. Fixed-flexion view X-ray of the knee superior in detection and follow-up of knee osteoarthritis. *Medicine*. 2017;96(49):e9126. doi:10.1097/MD.0000000000009126.
[12] Felson DT, Nevitt MC, Yang M, Clancy J, Niu JC. A new approach yields high rates of radiographic progression in knee osteoarthritis. *J Rheumatol*. 2008;1(35):2047–2054.
[13] Duddy J, Kirwan JR, Szebenyi B, Clarke S, Granell R, Volkov S. A comparison of the semiflexed (MTP) view with the standing extended view (SEV) in the radiographic assessment of knee osteoarthritis in a busy routine X-ray department. *Rheumatology*. 2005;44(3):349–351. doi:10.1093/rheumatology/keh476.
[14] Wolfe F, Lane NE, Buckland-Wright C. Radiographic methods in knee osteoarthritis: a further comparison of semiflexed (MTP), schuss-tunnel, and weight-bearing anteroposterior views for joint space narrowing and osteophytes. *J Rheumatol*. 2002;29(12):2597–2601.
[15] Duncan ST, Khazzam MS, Burnham JM, Spindler KP, Dunn WR, Wright RW. Sensitivity of Standing Radiographs to Detect Knee Arthritis: A Systematic Review of Level I Studies. *Arthroscopy*. 2015;31(2):321–328. doi:10.1016/j.arthro.2014.08.023.
[16] Vince AS, Singhania AK, Glasgow MMS. What knee X-rays do we need? A survey of orthopaedic surgeons in the United Kingdom. *Knee*. 2000;7(2):101–104. doi:10.1016/S0968-0160(00)00036-3.
[17] Bhatnagar S, Carey-Smith R, Darrah C, Bhatnagar P, Glasgow MM. Evidence-based practice in the utilization of knee radiographs—A survey of all members of the British Orthopaedic Association. *Int Orthop*. 2006;30(5):409–411. doi:10.1007/s00264-006-0099-6.
[18] Government UK. *The Ionising Radiation (Medical Exposure) Regulations 2017*. London: UK Statutory Instruments; 2017.
[19] Harrison JD., Balonov M., Bochund F., Martin C., Menzel HG., Ortiz-Lopez P., et al. ICRP publication 147: Use of dose quantities in radiological protection, 2021.
[20] International Commission on Radiological Protection. ICRP Publication 147. Editorial. Dose and risk: Science and protection. , 2021.
[21] Public Health England. National Diagnostic Reference Levels (NDRLs) , London; 2019.
[22] Health Protection Agency. HPA-CRCE-034: doses to patients from radiographic and fluoroscopic x-ray imaging procedures in the UK - 2010 review , London; 2012.
[23] Sanfridsson J, Holje G, Svahn G, Ryd L, Jonsson K. Radiation dose and image information in computed radiography: A phantom study of angle measurements in the weight-bearing knee. *Acta Radiol*. 2000;41(4):310–316. doi:10.1080/028418500127345541.
[24] College of Radiographers. Research Priorities for the radiographic profession: A Delphi Consensus Study, London; 2017.
[25] College of Radiographers. Research Strategy 2021-2026 , London; 2021.
[26] Tapiovaara M, Siiskonen T, Lakkisto M, Servomaa A. *A PC based Monte Carlo program for calculating patient doses in medical x-ray examinations*; 2008 Report STUK A—231(ED.2), Helsinki.
[27] Cristy M, Eckerman KF. *Specific absorbed fractions of energy at various ages from internal photon sources*; 1987 I. Methods. Report ORNL/TM-8381/V1, Oak Ridge.
[28] Stratakis AP J. *Chapter 1 Dosimetry. Radiation Dose Management of Pregnant Patients, Pregnant Staff and Paediatric Patients*. IOP Publishing; 2019.
[29] Hart D, Jones DG, Wall BF. *Normalised organ doses for medical x-ray examinations calculated using Monte Carlo techniques*. Chilton: NRPB-SR262; 1994.
[30] Hart D, Jones DG, Wall BF. *Normalised organ doses for paediatric x-ray examinations calculated using Monte Carlo techniques*. Chilton: NRP-B-SR279; 1996.
[31] Jones DG, Wall BF. *Organ doses from medical x-ray examinations calculated using Monte Carlo techniques*. Chilton: NRPB -R186; 1985.
[32] Jones DG, Wall BF. *Estimation of effective dose in diagnostic radiology from entrance surface dose and dose-area product measurements*; 1994 Report NRPB-R262, Chilton.
[33] International Commission on Radiological Protection. The 2007 Recommendations of the International Commission on Radiological Protection. *Annals of the ICRP*. 2007;103.
[34] National Research Council D on E and LSB on RERC to AHR from E to LL of IR. *Health Risks from Exposure to Low Levels of Ionizing Radiation*. Washington: The National Academies Press; 2006 BEIR VII..
[35] Vano E, Frija G, Loose R, Paulo G, Efstathopoulos E, Granata C, et al. Dosimetric quantities and effective dose in medical imaging: a summary for medical doctors. *Insights Imaging*. 2021;12(1):99. doi:10.1186/s13244-021-01041-2.
[36] Alderson SW, Lanzl LH, Rollins M, Spira J. An instrumented phantom system for analog computation of treatment plans. *Am J Roentgenol Radium Ther Nucl Med*. 1962;87:185–195.
[37] Fluke Biomedical LLC. *TNT 12000 system, (TNT 12000) DoseMate Dosimeter (Ion Chamber (96020C) 150cc*. (TNT 12000D) Wireless Display; 2010.
[38] Vosper M. Dosimetry 13.6-13.11 . In: Ramlaul A, editor. Medical Imaging and Radiotherapy Research: Skills and Strategies. 2nd ed., Springer International Publishing AG ; 2020, p. 243–51.
[39] Bos AJJ. High sensitivity thermoluminescence dosimetry. *Nucl Instrum Methods Phys Res B*. 2001;184(1–2):3–28. doi:10.1016/S0168-583X(01)00717-0.
[40] Whitley AS, Jefferson G, Holmes K, Sloane C, Anderson C, Hoadley G. *Clark's Positioning in Radiography 13E*. 13th ed. CRC Press; 2015.
[41] Siemens Healthineers AG. X-ray tube Opti 150/30/50HC-100 2009.
[42] AGFA Healthcare. NX3.0 Muscia Acquisition Workstation, AGFA DX-D 40C cassette 43 × 35cm 2015.
[43] Newell DB, Tiesinga E. *The international system of units (SI)*. MD: Gaithersburg; 2019.
[44] Landauer. ⅛" x ⅛" x 0.15" TLD-100H . TLD Chip: Single Point Radiation Assessments. Available from: https://www.landauer.co.uk/produit/tld-chip-single-point-radiation-assessments/[accessed October 4, 2022].
[45] Corredor CE. *Dose Analysis by Radiation Treatment Planning System (TPS) Software Vs*. Thermoluminescent Dosimeters Output. University of Tennessee; 2004.
[46] Thermo Electron Corporation. Thermo Fisher Scientific Harshaw TLD Model 5500 Reader with WinREMS Operator's Manual (5500-W-O-0805-006). , 2005.
[47] Omojola AD, Akpochafor MO, Adeneye SO, Aweda MA. Determination of Calibration Factors and Uncertainties Associated with the Irradiation of MTS-N (LiF: Mg, Ti) Chips with Cesium-137 and X-ray Sources Under Low Doses for Personal Dosimetry in Diagnostic Radiology. *Journal of Global Radiology*. 2021;7(1). doi:10.7191/jgr.2021.1103.
[48] Carbolite Gero. TLD/3 Rapid Cooling Oven n.d.
[49] Hanna DW *Development and optimization of a thermoluminescent dosimeter (TLD) analyser system for low-dose measurements utilizing photon counting techniques*. Kansas. Kansas State University; 1979.

Please cite this article as: P. Lockwood and M. Mitchell, An assessment of the dose and image quality difference between AP and PA positioned adult radiographic knee examinations, Journal of Medical Imaging and Radiation Sciences, https://doi.org/10.1016/j.jmir.2022.12.004

[50] Hasabelrasoul HA. *Estimation of uncertainty in TLD calibration*. Sudan Academy of Science; 2013.
[51] Saint-Gobain crystals and detectors. Thermo Fisher WinREMS software (v.PL-26732.8.1.0.0) 2012.
[52] Thermo Electron Corporation. Thermo Fisher Scientific Harshaw TLD Model 5500 Reader with WinREMS Operator's Manual (5500-0-S-0399-001-S1) , 2005.
[53] Hafezi L, Arianezhad SM, Hosseini Pooya SM. Evaluation of the radiation dose in the thyroid gland using different protective collars in panoramic imaging. *Dentomaxillofacial Radiology*. 2018;47(6):20170428. doi:10.1259/dmfr.20170428.
[54] Boyd WL. *Using Thermoluminescent Dosimeters to Measure the Dose From High and Low Energy X-Ray Sources*. Las Vegas: University of Nevada; 2009.
[55] Marshall G, Jonker L. An introduction to inferential statistics: A review and practical guide. *Radiography*. 2011;17(1):e1–e6. doi:10.1016/j.radi.2009.12.006.
[56] Carmichael JHE, Maccia C, Moores BM, Oestmann JW, Schibilla H, Teunen D, et al. *European guidelines on quality criteria for diagnostic radiographic images*. Office for Official Publications of the European Communities; 1996.
[57] Random.Org. Random Sequence Generator . Random Sequence Generator . Available from: https://www.random.org/sequences/[accessed October 10, 2022].
[58] Hakansson M, Svensson S, Zachrisson S, Svalkvist A, Bath M, Manssson LG. VIEWDEX: an efficient and easy-to-use software for observer performance studies. *Radiat Prot Dosimetry*. 2010;139(1–3):42–51. doi:10.1093/rpd/ncq057.
[59] Image Information Systems. *IQ-Web*. IQ-Web; 2022.
[60] Kheddache S, Mansson LG, Sund P, Bath M. Comparison of visual grading analysis and determination of detective quantum efficiency for evaluating system performance in digital chest radiography. *Eur Radiol*. 2004;14(1):48–58. doi:10.1007/s00330-003-1971-z.
[61] Metsälä E, Fridell K. Insights into the methodology of radiography science. *Radiography*. 2018;24(4):e105–e108. doi:10.1016/j.radi.2018.05.010.
[62] Precht H, Hansson J, Outzen C, Hogg P, Tingberg A. Radiographers' perspectives' on Visual Grading Analysis as a scientific method to evaluate image quality. *Radiography*. 2019;25:S14–S18. doi:10.1016/j.radi.2019.06.006.
[63] Toivonen M, Aschan C, Rannikko S, Karila K, Savolainen S. Organ Dose Determinations of X-Ray Examinations Using TL Detectors for Verification of Computed Doses. *Radiat Prot Dosimetry*. 1996;66(1):289–294. doi:10.1093/oxfordjournals.rpd.a031736.
[64] Campos de Oliveira PM, Squair PL, Lacerda MA, da Silva TA. Assessment of organ absorbed doses in patients undergoing chest X-ray examinations by Monte Carlo based softwares and phantom dosimetry. *Radiat Meas*. 2011;46(12):2073–2076. doi:10.1016/j.radmeas.2011.06.058.
[65] Schultz FW, Geleijns J, Spoelstra FM, Zoetelief J. Monte Carlo calculations for assessment of radiation dose to patients with congenital heart defects and to staff during cardiac catheterizations. *Br J Radiol*. 2003;76(909):638–647. doi:10.1259/bjr/21647806.
[66] Lee C, Park B, Lee SS, Kim JE, Han SS, Huh KH, et al. Efficacy of the Monte Carlo method and dose reduction strategies in paediatric panoramic radiography. *Sci Rep*. 2019;9(1):9691. doi:10.1038/s41598-019-46157-0.
[67] Health Protection Agency. *Radiation Risks from Medical X-Ray Examinations as a Function of the Age and Sex of the Patient*. Chilton: (HPA-CRCE-028); 2011.
[68] Health Protection Agency. Risks from Ionising Radiation. (HPA-RPD-066), Chilton; 2010.

Please cite this article as: P. Lockwood and M. Mitchell, An assessment of the dose and image quality difference between AP and PA positioned adult radiographic knee examinations, Journal of Medical Imaging and Radiation Sciences, https://doi.org/10.1016/j.jmir.2022.12.004